Properties of Polycarbonate/Acrylonitrile-Butadiene-Styrene/Talc Composites

Y. T. Sung,[1] P. D. Fasulo,[2] W. R. Rodgers,[2] Y. T. Yoo,[3] Y. Yoo,[1] D. R. Paul[1]

[1]*Department of Chemical Engineering and Texas Material Institute, The University of Texas at Austin, Austin, Texas 78712-1062*
[2]*General Motors Research and Development Center, Warren, Michigan 48090*
[3]*Department of Materials Chemistry and Engineering, Konkuk University, Seoul 143-701, Republic of Korea*

Received 18 May 2011; accepted 24 June 2011
DOI 10.1002/app.35147
Published online 11 October 2011 in Wiley Online Library (wileyonlinelibrary.com).

ABSTRACT: The morphology, tensile, impact properties, and thermal expansion behavior of polycarbonate (PC)/acrylonitrile-styrene-butadiene (ABS)/talc composites with different compositions and mixing sequences were investigated. From the studies of morphology of the PC/ABS/talc composites, it was observed that some talc particles were located in both the PC and the ABS phases of the blend but most were at the interface between the PC and ABS phases for every mixing sequence. Aspect ratios of the talc particles determined by TEM image analysis reasonably matched values computed from tensile modulus using composite theory. The thermal expansion behavior, or CTE values, was not significantly influenced by the mixing sequence. The impact strength of the PC/ABS/talc composites depended significantly on the mixing sequence; a premix with PC gave the poorest toughness. The molecular weight of the PC in PC/talc composites was found to be significantly decreased. It appears that the impact strength of the PC/ABS/talc composites is seriously compromised by the degradation of the PC caused by talc. © 2011 Wiley Periodicals, Inc. J Appl Polym Sci 124: 1020–1030, 2012

Key words: polycarbonate; acrylonitrile-styrene-butadiene; talc; composite; impact strength

INTRODUCTION

Fillers are frequently added to polymers to improve mechanical and thermal performance. Polymer composites based on talc as the filler are in wide-scale use for many applications. Talc is a trioctahedral 2 : 1 layer silicate mineral, characterized by three octahedral Mg positions per four tetrahedral Si positions.[1–3] Talc can increase stiffness, reduce mold shrinkage, and decrease the thermal expansion of polymer composites.[3–7]

Polymers are frequently considered by the automotive industry for replacement of metals because of the ease of fabrication and the reduction in weight that can be achieved. However, the high linear coefficient of thermal expansion (CTE) of polymers leads to problems caused by mismatch of CTE with other components.[8–12] For polycarbonate (PC)/acrylonitrile-styrene-butadiene (ABS) blends, CTE is frequently an important problem and some commercial PC/ABS blends with low CTE have been claimed.[13,14]

Adding talc to PC/ABS blends can be a promising way to reduce the CTE of PC/ABS blends. Addition of talc can lower the CTE by volume dilution with a material of lower CTE and by mechanical constraint by a high aspect ratio filler with low CTE and high modulus. Some mechanical properties such as tensile modulus can be increased by addition of talc.

However, when talc is added to PC/ABS blends, the toughness must also be considered. In general, there is trade-off between stiffness and toughness in polymer/filler composites. Also, a significant decrease in molecular weight of PC may occur by degradation when certain fillers are added to the PC matrix; this can be another cause of decreased toughness.[15]

In this article, we present the morphology, tensile, impact properties and thermal expansion behavior of PC/ABS/talc composites prepared by different sequences of melt mixing of the various components. In particular, changing the mixing sequence can be useful for understanding how the properties of the PC/ABS blend/talc composites can be altered. Also, the effects of talc on the molecular weight degradation of PC are considered.

EXPERIMENTAL

Materials and composites preparation

The PC and ABS used in this study were Dow Calibre 200-22 and Magnum 1040. Magnum 1040 is a mass-made ABS which is evident from the TEM

Correspondence to: D. R. Paul (drp@che.utexas.edu).
Contract grant sponsors: General Motors.

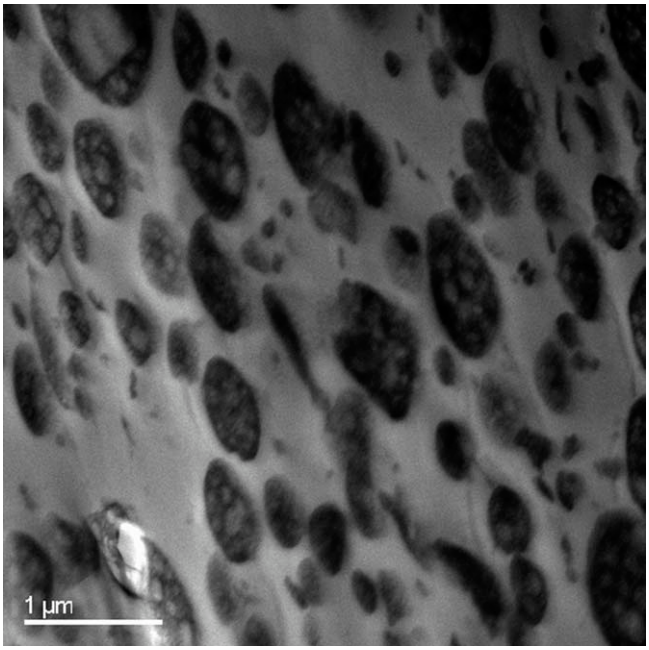

Figure 1 TEM micrograph of ABS used in this study.

image shown in Figure 1; it is reported to have a high rubber content. The properties of the PC and ABS are summarized in Table I along with the properties of a commercial low CTE PC/ABS/talc composite for comparison. The talc used in this study is HTP Ultra 5c which is supplied by IMIFABI S.p.A, Benwood, WA, USA.

The PC/talc (90/10 wt %), ABS/talc (90/10 wt %), and PC/ABS/talc composites were extruded using a Haake corotating, intermeshing twin screw extruder. The detailed extrusion conditions are summarized in Table II. Also, the PC and ABS controls were extruded to achieve comparable thermal history. For the PC/ABS/talc composites, a filler content of 10 wt % was chosen to mix with the PC/ABS matrix. The PC content in the PC/ABS matrix was set at 30, 50, and 70 wt %. The extrusion of the PC/ABS/talc composites was performed using one-step and two-step sequences. In the one-step extrusion, all components were added simultaneously to the extruder.

TABLE II
Detailed Extrusion Conditions for Composites

	Temperature (°C)	RPM	Feed rate (kg h^{-1})
PC/talc composites	260	280	1
ABS/talc composites	220	280	1
PC/ABS/talc composites	260	280	1

For the two-step extrusion, PC/talc or ABS/talc masterbatches were prepared first. Then the appropriate masterbatch was extruded with the second polymer. The formulations of the extruded samples are summarized in Figure 2. All samples were dried in a vacuum oven at 80°C for at least 16 h.

The Izod and tensile specimens were prepared using an Arburg Allrounder 305-210-700 injection molding machine. The temperature of the barrel and die were set at 270°C for PC, 280°C for the PC/talc composite, 220°C for ABS, 230°C for the ABS/talc composite, and 270°C for the PC/ABS/talc composites. In all cases, the injection and holding pressures were set at 80 and 35 bar, respectively. All polymer samples were dried in a vacuum oven at 80°C for at least 16 h prior to any melt processing.

Morphology characterization

Ultrathin sections for transmission electron microscopy (TEM) were prepared using a diamond knife under cryogenic conditions. When microtoming ABS, ABS/talc, and PC/ABS/talc materials, the specimen temperature was set at −65°C, while the knife temperature was set at −58°C. To help identify the polymer phases in the TEM images, osmium tetroxide (OsO_4) was used to stain the rubber particles black while ruthenium tetraoxide (RuO_4) was used to stain the PC phase gray. Sections of ABS and ABS/talc materials were vapor strained for 18 h using a 2.0% aqueous solution of osmium tetroxide (OsO_4). Sections of PC/ABS/talc composites were first exposed to OsO_4 for 18 h then exposed to 0.5% RuO_4 for 8 min. This dual staining technique allows

TABLE I
Properties of PC and ABS Used in this Study

	PC	ABS	Commercial PC/ABS/talc composite
Designation	Dow Calibre 200-22	Dow Magnum 1040	GE CYCOLOY XCM 850
Tensile modulus (GPa)	2.44	2.19	5.16
Tensile strength (MPa)	61.5	48.7	67.1
Strain at break (%)	80.7	10	17.6
Impact strength (J m^{-1})	713	416	251
CTE in flow direction (10^{-5} mm mm^{-1} °C^{-1})	6.7	8.3	4.2
CTE in transverse direction (10^{-5} mm mm^{-1} °C^{-1})	6.7	9.2	5.5
CTE in normal direction (10^{-5} mm mm^{-1} °C^{-1})	6.8	10.3	9.0

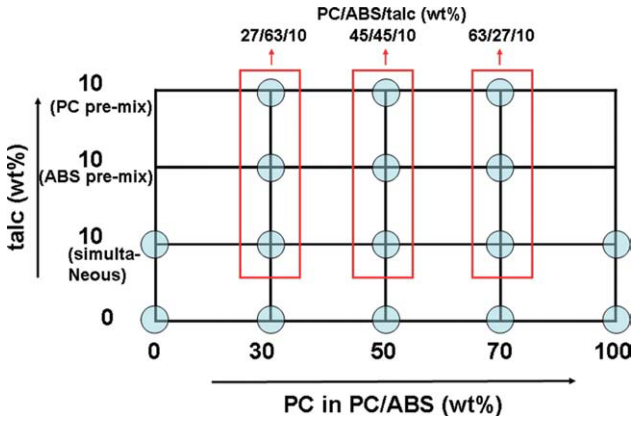

Figure 2 Experimental plan for examining PC/ABS/talc composites. [Color figure can be viewed in the online issue, which is available at wileyonlinelibrary.com.]

simultaneous viewing of the PC, SAN, butadiene rubber, and talc. Finding the optimal staining time is critical to avoid artifacts from overstaining when using RuO_4. A JEOL 2010 F TEM was used at 120-kV voltage. Also, the samples without staining were used for the image analysis.

Particle analysis

The samples without staining were used for the image analysis of talc particles. TEM images, typically 2000× in magnification were used for this analysis. Detailed procedures for image analysis are described in previous papers.[10,16]

Mechanical properties

Tensile properties were obtained using an Instron model 1137 according to ASTM D 638. Tensile modulus was determined with the use of an extensometer at a crosshead speed of 0.51 mm min^{-1}. Yield properties were determined at a crosshead speed of 5.1 mm min^{-1}. Tensile properties reported here represent an average from at least five specimens.

Izod impact tests were performed using a pendulum-type tester. Standard notch test bars (thickness = 3.18 mm) conformed to ASTM D 256. The values reported here represent an average from at least five specimens.

Thermal expansion behavior

Linear coefficients of thermal expansion, CTE, were measured using a Perkin–Elmer thermomechanical analyzer according to ASTM D696. CTE values for molded bars were measured along the flow direction (FD). The procedure of measurement was as follows: the specimen was held at −40°C for 5 min, followed by heating at a rate of 5°C min^{-1} to 80°C and held for 30 min. Then the sample was quenched to room temperature. After storage at room temperature for at least one day, a second heating of the sample was done at a rate of 5°C min^{-1} from −40 to 80°C. The CTE value was determined between 20 and 50°C during the second heating.

Viscometry

The dilute solution viscosity of the PC in PC/talc composites was measured at 25°C in 0.5% (w/v) chloroform solutions using an Ubbelohde viscometry. Before viscometry measurements, the samples were filtered using a syringe filter. The intrinsic viscosity was determined by a single point method using the Solomon-Ciuta (SC) equation[17–19]

$$[\eta] = [2\{t/t_0 - \ln(t/t_0) - 1\}]^{1/2}/c \quad (1)$$

where [η] is the intrinsic viscosity, c is the concentration of the PC in the solution, t is the flow time for the PC solution, and t_0 is the flow time for pure solvent. For the determination of molecular weight M, the following equation[20] was used

$$[\eta] = 12.0 * 10^{-3} M^{0.82} \quad (2)$$

Thermal analysis

Thermal properties of samples were measured using a Perkin–Elmer differential scanning calorimeter, model DSC-7. Scans were made from 50 to 220°C at a heating rate of 10°C min^{-1} and held for 3 min to eliminate thermal history. Then the sample was cooled to 50°C at a rate of 10°C min^{-1}. After cooling, a second heating was made from 50 to 220°C at a heating rate of 10°C min^{-1}. The glass transition (T_g) was determined from the second heating.

RESULTS AND DISCUSSION

Morphology

Figure 3 shows TEM images of PC/ABS/talc composites where the PC/ABS ratio = 70/30 and the talc content = 10 wt %. To identify the location of the talc in the PC/ABS/talc composites, the TEM specimens were stained with OsO_4 and RuO_4. After staining, the PC, SAN, and butadiene phases appeared gray, white, and black, respectively. From Figure 3(a), we see that, for the PC/ABS (70/30 wt %) blend without talc, the ABS forms an elongated dispersed phase. When the talc is added to the PC/ABS matrix using simultaneous mixing [Fig. 3(b)], the talc particles exist in the PC, in the ABS and at the interface between PC and ABS. A similar particle distribution was observed for the samples made by

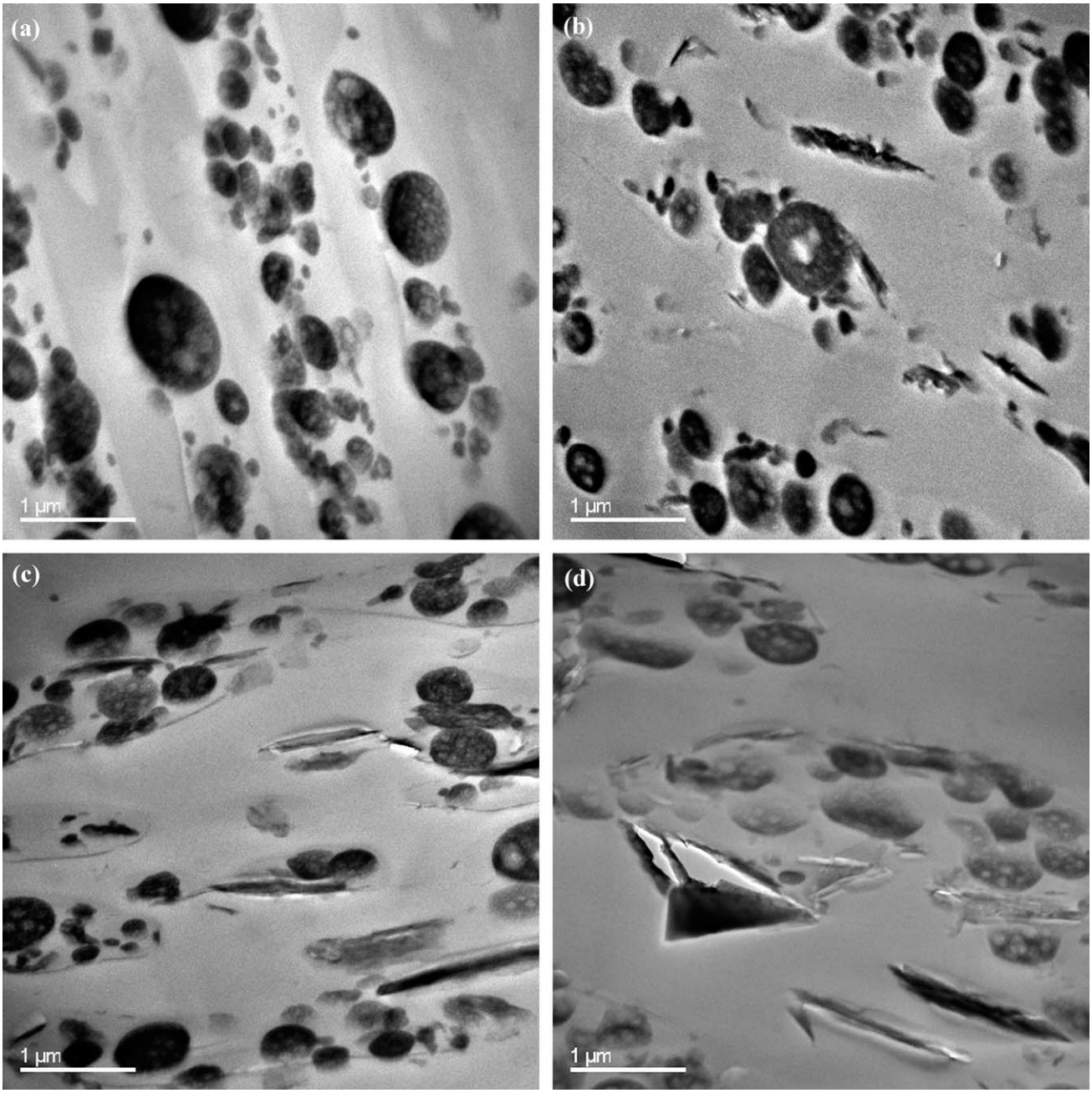

Figure 3 TEM micrographs of PC/ABS/talc composites (talc = 10 wt %, PC in PC/ABS blend = 70 wt %): (a) no talc; (b) simultaneous; (c) ABS premix; (d) PC premix. The talc particles are long and rectangular in shape while the rubber particles from the ABS are oval shaped.

two-step mixing [Fig. 3(c,d)]. However, it was noted that the talc particles exist mainly at the interface between PC and ABS for both mixing sequences. The purpose for changing the mixing sequence was to determine if this is a useful way to alter the morphology of the PC/ABS/talc composites. However, from Figure 3, it is observed that the differences in talc location among the different mixing sequences used are not significant even though the size of the dispersed phase (ABS) is changed which may be due to the change of the viscosity ratio. Figure 4 shows a schematic representation of the morphology for the PC/ABS/talc composite where the talc content is 10 wt % and the PC/ABS ratio = 70/30.

Figure 5 shows TEM images of PC/ABS/talc composites containing 10 wt % talc where the PC/ABS ratio = 30/70. Figure 5(a) shows that PC is the dispersed phase in the PC/ABS blend without talc. When talc is added using simultaneous mixing [Fig. 5(b)] or two-step mixing [Fig. 5(c,d)], the talc particles exist in the PC, in the ABS and at the interface between PC and ABS. Again, it is observed that the

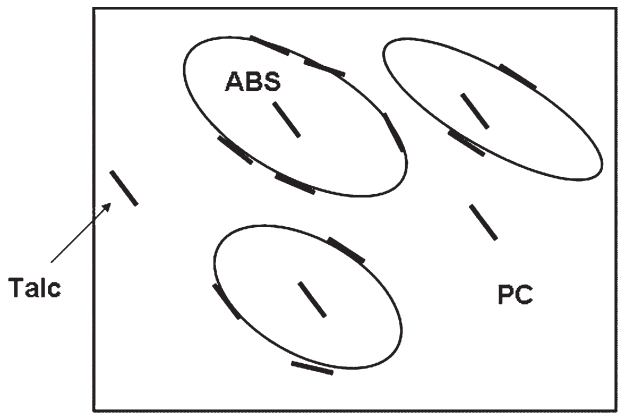

Figure 4 Schematic of morphology of the PC/ABS/talc composites (talc = 10 wt %, PC in PC/ABS blend = 70 wt %).

difference in talc location among the different mixing sequences used is not significant. For both PC/ABS ratios of 70/30 (Fig. 3) and 30/70 (Fig. 5), the talc exists mainly at the interface between the PC and ABS for both mixing sequences.

The location of filler particles (Component 3) in an immiscible blend of Polymers 1 and 2 can be predicted by analysis of the relative interfacial tensions, γ_{ij}, of the components. The value of the ratio $(\gamma_{13} - \gamma_{23})/\gamma_{12}$ determines the equilibrium location of the filler particles.[21,22] When this ratio is greater than +1, the filler particle prefers to be located in Polymer 2. When this ratio is less than −1, the particle prefers to be in Polymer 1. However, when this ratio is between −1 and 1, the particles are trapped at the interface between the two polymer phases.[21,22]

To calculate the three interfacial tensions for the PC, ABS (or SAN) and talc system the following equation was used

$$\gamma_{ij} = \gamma_i + \gamma_j - \frac{4\gamma_i^d\gamma_j^d}{\gamma_i^d + \gamma_j^d} - \frac{4\gamma_1^d\gamma_2^d}{\gamma_1^d + \gamma_2^d} \quad (3)$$

where γ_{ij} is the interfacial tension, γ_i and γ_j are the surface tension, γ^d and γ^p are the dispersion and polar components, respectively, where the subscripts i and j refer to the two individual phases. Values of the various parameters in eq. (3) was obtained from the literature and interfacial tensions were computed from them. The results are shown in Table III. Also, from Table III, the value of $(\gamma_{13} - \gamma_{23})/\gamma_{12}$ is seen to be 0.7, which is consistent with the results that talc particles exist mainly at the interface between the PC and ABS phase as seen in Figures 3–5. From Figures 3 to 5 and Table III, it is suggested that the affinities of PC and of ABS for the surface of talc are rather similar. Therefore, talc appears to prefer being at the interface between PC and ABS for every mixing sequence.

Particle analysis

Figure 6 shows a typical histogram of the distribution of the length and aspect ratio of the talc particles obtained from analysis of TEM images of a composite containing 10 wt % of talc in a blend where the PC/ABS ratio = 50/50 that was formed by the simultaneous mixing process. This analysis was performed using TEM images of samples without staining as explained earlier.

Table IV shows image analysis results of talc particles from TEM images for PC/ABS/talc composites with different PC/ABS ratios and formed by different mixing sequences. In Table IV, we show four different aspect ratios i.e., $\langle l/t\rangle_n$ and $\langle l/t\rangle_w$ based on averaging aspect ratios determined for individual talc particles; $\overline{l_n}/\overline{t_n}$ and $\overline{l_w}/\overline{t_w}$ based on averaging the length and the thickness separately for the talc particle distribution. From Table IV, it is shown that the aspect ratios calculated by averaging the values for each particle, $\langle l/t\rangle_n$ and $\langle l/t\rangle_w$ are always larger than those calculated from the ratio of the average talc length and thickness, $\overline{l_n}/\overline{t_n}$ and $\overline{l_w}/\overline{t_w}$. In general, the aspect ratio of the talc particles tends to decrease as the PC content decreases; this is especially clear from the ratio of the average talc length and thickness ($\overline{l_n}/\overline{t_n}$ or $\overline{l_w}/\overline{t_w}$). This tendency is shown graphically in Figure 7 and appears to be more or less independent of the mixing sequence. The decrease of the aspect ratio can be affected by several factors such as the different melt viscosities of the PC and ABS. However, determining the cause for these trends was beyond the scope of this work.

Tensile properties

Figure 8 shows the tensile modulus for PC/ABS/talc composites. The tensile modulus of the pure PC is 2.44 GPa while the value for the neat ABS is 2.19 GPa. The modulus of the PC/ABS blends is intermediate to those of the pure components. When talc is added to the PC/ABS matrix, the tensile modulus increases as expected.

The increase in the tensile modulus caused by addition of talc can be understood in terms of the Halpin-Tsai equations[25,26]

$$\frac{E}{E_m} = \frac{1 + 2\rho\eta\phi}{1 - \eta\phi} \quad (4)$$

where

$$\eta = \frac{E_p - E_m}{E_p + 2\rho E_m} \quad (5)$$

In these equations, E is the tensile modulus of the composite; E_m is the tensile modulus of the matrix;

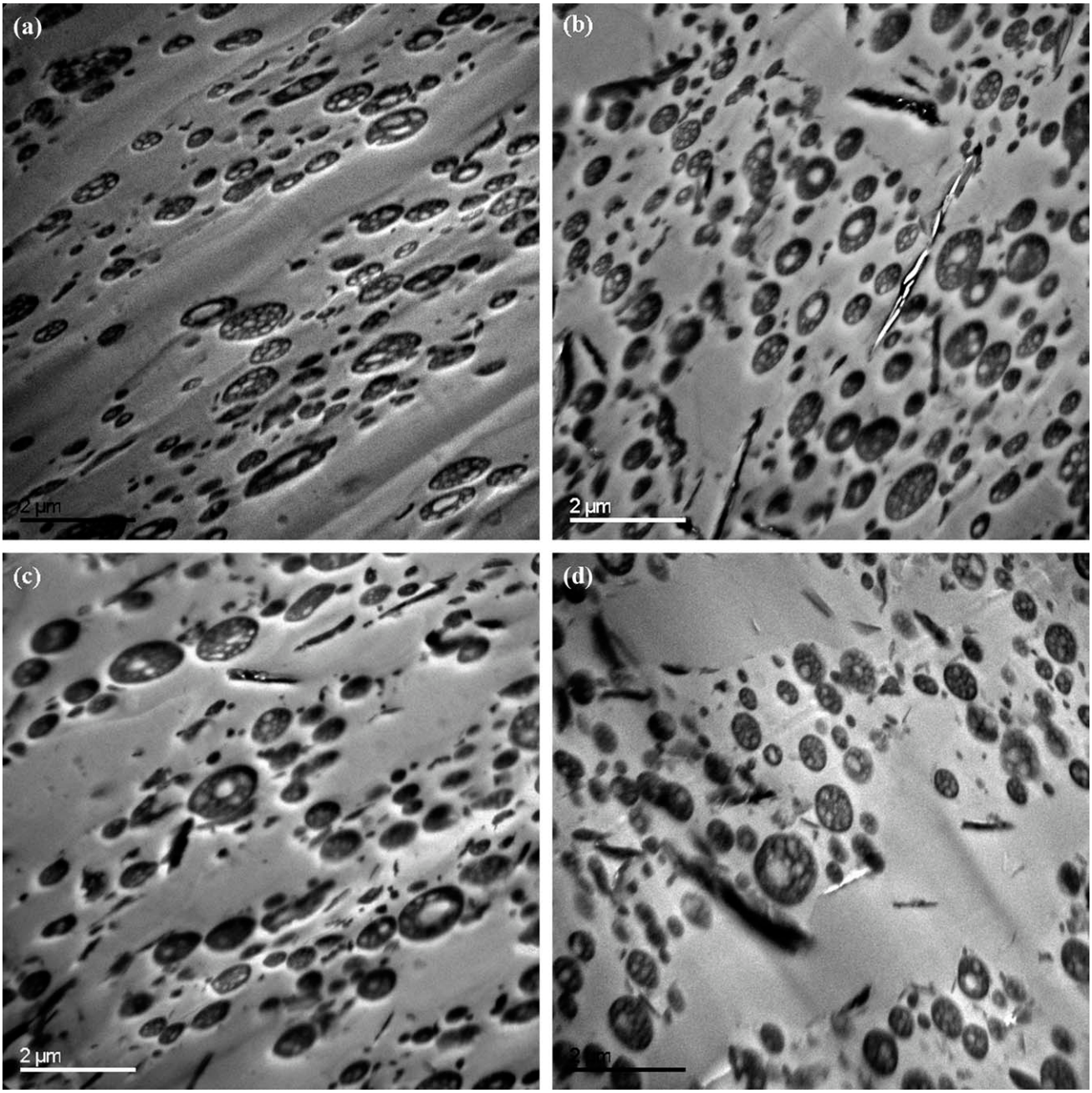

Figure 5 TEM micrographs of PC/ABS/talc composites (talc = 10 wt %, PC in PC/ABS blend = 30 wt %): (a) no talc; (b) simultaneous; (c) ABS premix; (d) PC premix. The talc particles are long and rectangular in shape while the rubber particles from the ABS are oval shaped.

TABLE III
Morphology Prediction from Analysis of Surface Forces

Subscripts			Surface tension (dispersion) (mN m^{-1})			Surface tension (polar) (mN m^{-1})			Interfacial tension (mN m^{-1})			
1	2	3	γ_1^d	γ_2^d	γ_3^d	γ_1^p	γ_2^p	γ_3^p	γ_{12}	γ_{23}	γ_{13}	$(\gamma_{13}-\gamma_{23})/\gamma_{12}$
PC	ABS	Talc	21.5[a]	19.7[a]	53.0[b]	7[a]	4.6[a]	0.1[b]	0.6	19.6	20.0	0.7

[a] DATA from academic paper.[23]
[b] DATA from academic paper.[24]

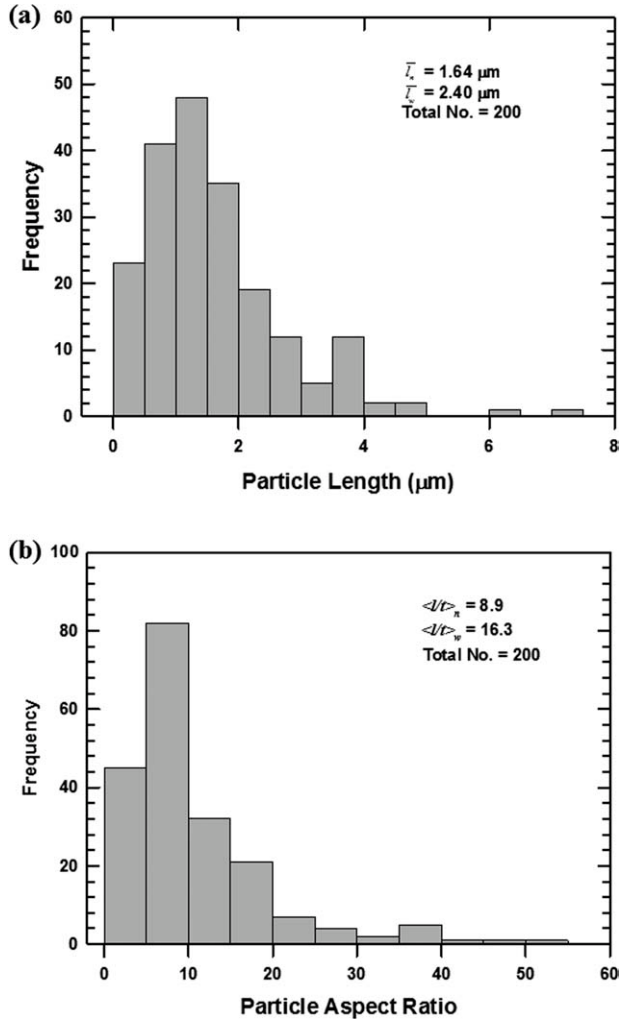

Figure 6 Histogram of talc particle length and aspect ratio in PC/ABS/talc composites (talc = 10 wt %, PC in PC/ABS blend = 50 wt %, simultaneous addition of all compounds).

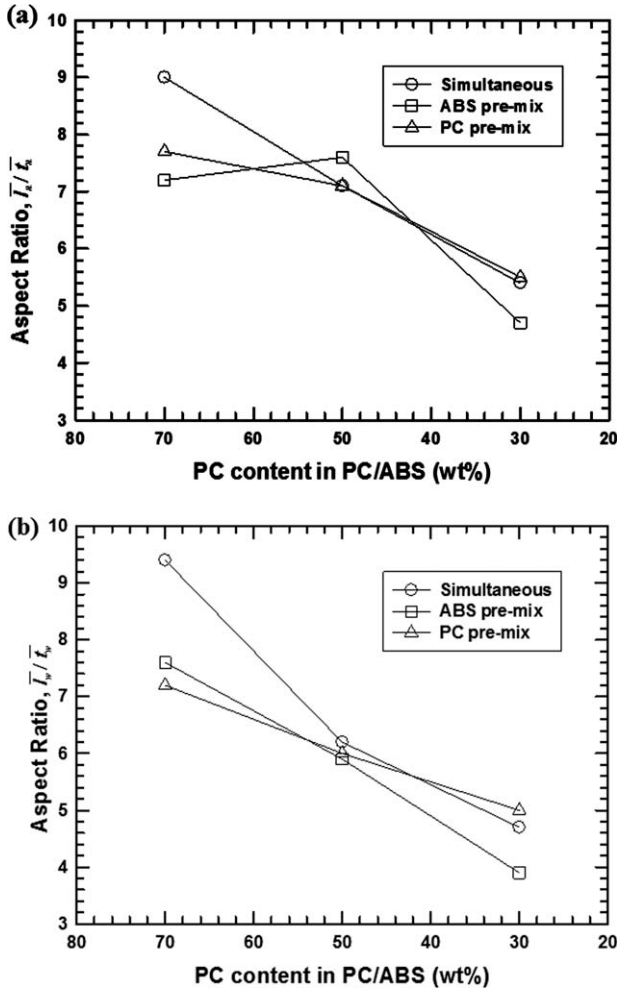

Figure 7 Aspect ratio of the PC/ABS/talc composites: (a) aspect ratio calculated from number average particle dimensions; (b) weight average particle dimensions.

TABLE IV
Image Analysis Results of Talc Particles from TEM Images for PC/ABS/Talc Composites with Different PC Content and Mixing Sequence

	PC content in PC/ABS								
	70			50			30		
	Simultaneous	ABS premix	PC premix	Simultaneous	ABS premix	PC premix	Simultaneous	ABS premix	PC premix
Number average particle length (μm), $\bar{l}_n$	1.25	1.17	1.03	1.64	1.47	1.16	1.14	1.23	1.13
Weight average particle length (μm), $\bar{l}_w$	1.89	1.88	1.41	2.41	2.27	1.70	1.67	2.20	1.66
Number average particle thickness (μm), $\bar{t}_n$	0.14	0.16	0.13	0.22	0.19	0.16	0.21	0.26	0.20
Weight average particle thickness (μm), $\bar{t}_w$	0.20	0.25	0.20	0.39	0.38	0.28	0.36	0.56	0.33
Number average aspect ratio, $\langle l/t \rangle_n$	12.2	10.2	9.7	8.9	9.0	10.4	7.9	7.9	8.9
$\bar{l}_n/\bar{t}_n$	9.0	7.2	7.7	7.1	7.6	7.1	5.4	4.7	5.5
Weight average aspect ratio, $\langle l/t \rangle_w$	15.5	15.2	12.5	16.3	14.9	14.9	16.6	15.0	14.5
$\bar{l}_w/\bar{t}_w$	9.4	7.6	7.2	6.2	5.9	6.0	4.7	3.9	5.0

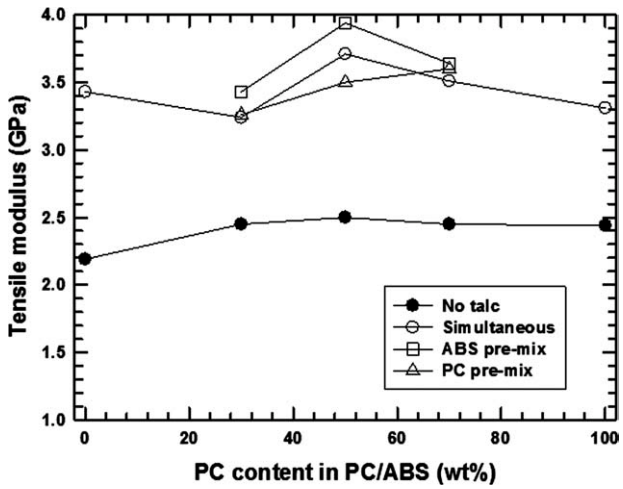

Figure 8 Tensile modulus of PC/ABS/talc composites.

E_P is the tensile modulus of the filler; ρ is the aspect ratio of the filler; ϕ is the volume fraction of the filler.

Figure 9 compares the experimental relative tensile moduli of the PC/ABS/talc composites with that predicted by the Halpin–Tsai equations. The modulus of talc and HAR-talc (E_P) was obtained from the literature (120.7 GPa).[27] The experimental results correspond to composites containing 10 wt % talc prepared by the mixing sequence indicated. Figure 9(a) shows results for a PC/ABS ratio of 70/30, Figure 9(b) for a ratio of 50/50 and Figure 9(c) for a ratio of 30/70. As seen in Figure 9, the experimental values of the normalized modulus lie between the lines predicted by the Halpin–Tsai equation with aspect ratios of 5 and 10 for PC/ABS ratios of 70/30 and 50/50; however, for the PC/ABS ratio of 30/70, the experimental data are better described by predictions using a lower aspect ratio, see Figure 9(c). These aspect ratios and trends with matrix compositions are entirely consistent with the experiment aspect ratios obtained by TEM, see Table IV and Figure 7, particularly when the ratios of average talc length and thickness, i.e., $\overline{l_n}/\overline{t_n}$ and $\overline{l_w}/\overline{t_w}$, are used.

Thermal expansion behavior

Figure 10(a) shows CTE values for PC/ABS blends and corresponding talc containing composites measured in the flow direction (FD). Values of CTE for the PC/ABS blends without talc are intermediate to those of the pure components. When 10% talc is added, the CTE is decreased by 25–30%. There are no significant differences in CTE resulting from the different mixing sequences used.

Figure 10(b) shows CTE values measured in the transverse direction (TD). For PC, the CTE in the TD direction is very similar to the value in the FD direction. However, for ABS the TD value is somewhat higher than that in the FD value. The anisotropy of the CTE of ABS may be due to orientation of the

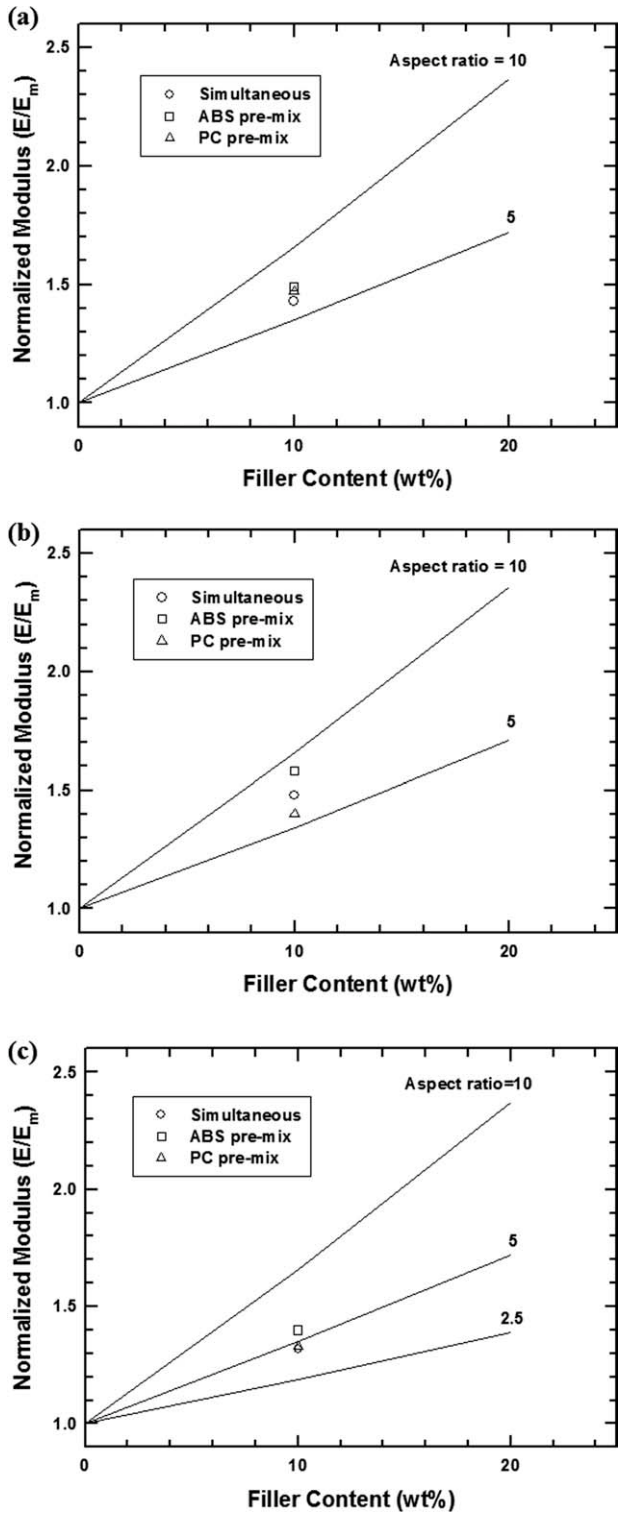

Figure 9 Comparison of theoretical tensile modulus predicted by Halpin-Tsai theory with experimental data of PC/ABS/talc composites: (a) PC in PC/ABS blend = 70 wt %; (b) PC in PC/ABS blend = 50 wt %; (c) PC in PC/ABS blend = 30 wt %.

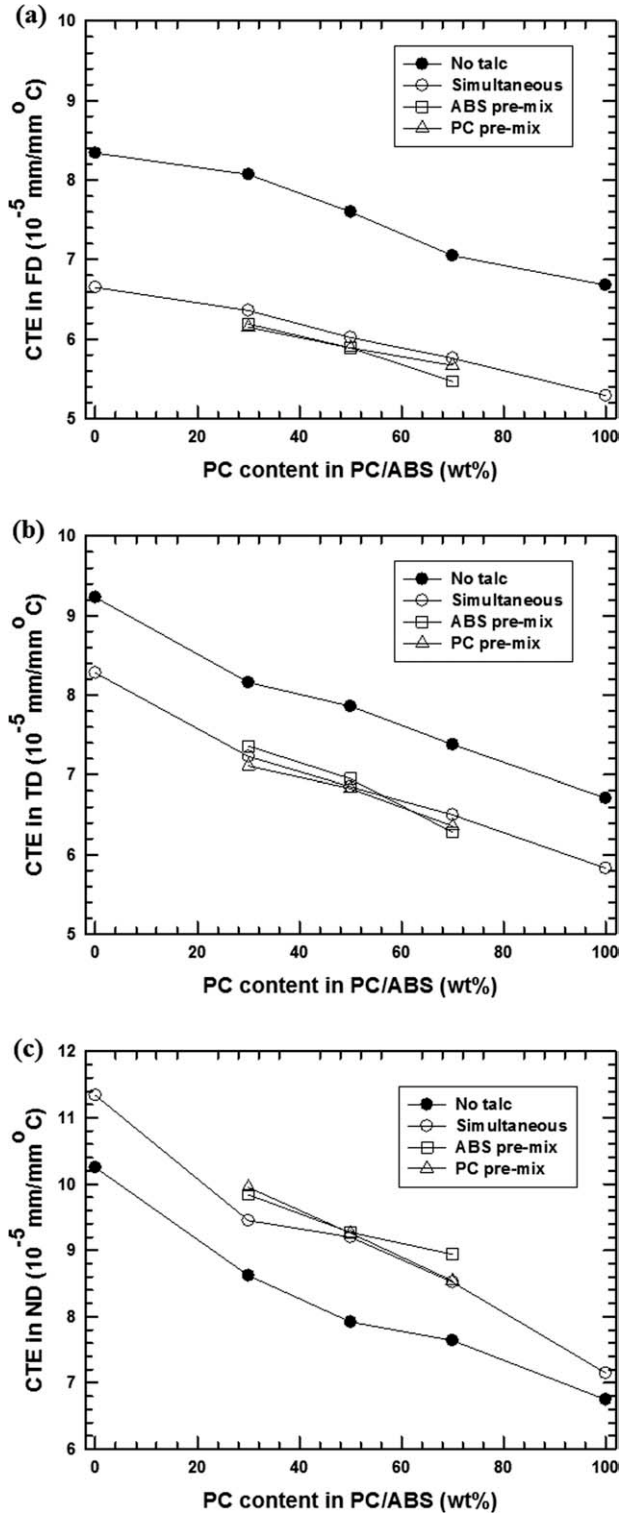

Figure 10 CTE of PC/ABS/talc composites (20 ~ 50°C): (a) FD direction; (b) TD direction; (c) ND direction.

complex morphology of ABS (Fig. 1) induced by molding. For the PC/ABS blends without talc, the CTE in the TD direction are intermediate to those of the pure components. When 10% talc is added to PC/ABS, the CTE in the TD direction is decreased by about 10–15%; the decrease in the CTE in the TD direction caused by adding talc is less than observed for the FD. Again, mixing sequence has no significant effect on the CTE in the transverse direction.

TABLE V
Impact Strength of PC/ABS/Talc Composites

	Impact strength (J m^{-1})				
	PC content in PC/ABS				
Filler content (wt %)	100	70	50	30	0
0 (no talc)	713	588	554	460	416
10 (simultaneous)	49	87	69	68	110
10 (ABS premix)	–	92	134	77	–
10 (PC premix)	–	38	29	31	–

Figure 10(c) shows CTE values measured in the ND direction. From Figure 10(c), the CTE of ABS in the ND direction is about 50% higher than that of PC. For the PC/ABS blends without talc, the CTE in the ND direction are intermediate to those of the pure components. When talc is added to PC/ABS blends, the CTE in the ND direction is increased. Similar results were reported by our laboratory for the nylon/clay,[28] PP/clay,[10] and TPO/clay nanocomposites.[9] The CTE in the ND direction is not significantly affected by mixing sequence.

The CTE of neat PC is nearly the same in all directions; whereas, for neat ABS the values rank in the order ND > TD > FD. The addition of talc lowers the CTE more in the FD than in the TD for all materials. The effect of the PC/ABS ratio on CTE for the talc containing composites is similar to that of the blends without talc.

Impact strength

Table V and Figure 11 show the impact strength of PC/ABS/talc composites. The impact strength of the PC/ABS blends is intermediate to those of the pure

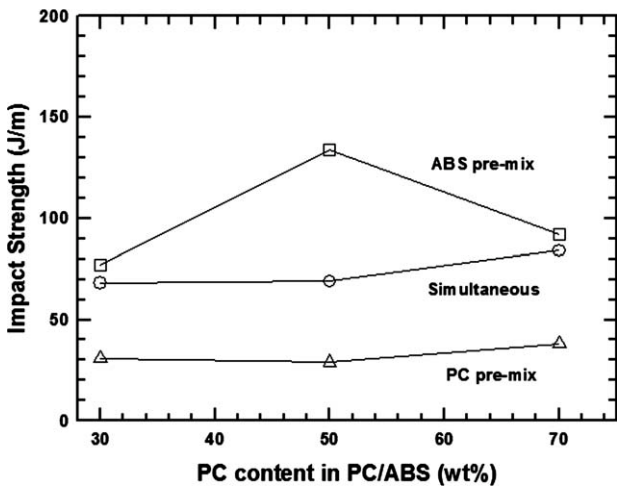

Figure 11 Comparison of impact strength of the PC/ABS/talc composites made by different mixing sequences.

TABLE VI
Molecular Weight of the PC and PC/Talc Composites from Intrinsic Viscosity Analysis

Samples	Intrinsic Viscosity (dL g^{-1})	Molecular weight (g mol^{-1})
PC (as-received)	0.44	22,400
PC (after extrusion)	0.44	22,300
PC/talc (90/10 wt %) composites	0.39	19,200
PC/talc (86/14 wt %) composites	0.35	16,800
PC/talc (82/18 wt %) composites	0.34	16,100
PC/talc (73/27 wt %) composites	0.32	14,900

components. When talc is added, the impact strength is dramatically decreased. The impact strength of the PC/ABS/talc composites is significantly altered by the mixing sequence. For example, the impact strength of the PC/ABS/talc composites show a much higher value when made by premixing the talc with the ABS first (134 J m^{-1}) than when the same composition is made by premixing the talc with PC (29 J m^{-1}). Simultaneous addition of the components gives an intermediate result. The low impact strength of the PC/ABS/talc composites may be influenced by several factors. One is, of course, the loss of ductility expected when fillers are added. However, as shown next, talc like some other fillers[14,29] causes molecular weight degradation of PC. A longer exposure of PC to talc in the melt state can be expected to cause greater degradation.

Molecular weight and thermal analysis

Table VI shows the molecular weight of PC after forming composites with talc as determined from intrinsic viscosity analysis. In Table VI, the PC/talc (86/14 wt %), PC/talc (82/18 wt %), and (73/27 wt %) composites correspond to the masterbatches used to make the PC/ABS/talc composites by two-step mixing using premix with PC. Table VI shows that the molecular weight of the PC is decreased as the talc content is increased. This significant decrease in the molecular weight of the PC reflects some chemistry induced by the talc and explains part of the decrease in the impact strength of PC/ABS/talc composites.

Table VII shows the glass transition temperature (T_g) of the PC/ABS/talc composites. For the PC/talc (90/10 wt %) composites, when talc is added, a significant decrease in the T_g observed, i.e., T_g goes from 146.0 to 139.0°C while the glass transition temperature of the ABS/talc (90/10 wt %) composites increases slightly from 107.0 to 108.9°C. From Table VII, when the talc is added to the PC/ABS matrix using two-step mixing with PC premix, a decrease of in the T_g of PC is observed that probably stems from the decrease of the PC molecular weight shown in Table VI.

CONCLUSIONS

In this study, the morphology, impact, tensile properties, and thermal expansion behavior of PC/ABS/talc composites made by different mixing sequences were investigated. TEM images showed that talc particles existed in the PC, in the ABS and at the interface between PC and ABS regardless of the mixing sequence; however, the majority of the talc particles existed mainly at the interface between PC and ABS for every mixing sequence which was consistent with an analysis of the interfacial forces. The talc particle aspect ratios determined experimentally varied with the PC/ABS ratio. The trends of tensile modulus agree with predictions by composite theory using the observed aspect ratios. Addition of talc reduced the CTE of the PC/ABS blends measured in the flow and transverse direction, but values in the normal direction were increased by addition of talc. Modulus and CTE values were not significantly affected by the mixing sequence used.

The impact strength of PC/ABS blends was significantly reduced by addition of talc. A portion of this decrease stems from chemical degradation of the PC caused by the talc as revealed by intrinsic viscosity

TABLE VII
DSC Analysis of PC/ABS/Talc Composites

	T_g (°C)									
	PC content in PC/ABS									
	100		70		50		30		0	
Filler content (wt %)	PC	ABS	PC	ABS	PC	ABS	PC	ABS	PC	ABS
0 (no talc)	146.0	–	142.4	109.7	141.4	109.5	140.0	107.5	–	107.0
10 (simultaneous)	139.0	–	140.5	108.5	138.6	107.0	138.7	107.5		108.9
10 (ABS premix)	–	–	140.6	108.9	138.6	108.9	138.9	108.0	–	–
10 (PC premix)	–	–	136.5	109.6	136.6	109.3	134.1	108.6	–	–

measurements. The impact strength of the PC/ABS/talc composites showed the lowest value when the premix with PC was used.

The authors thank General Motors for permission to publish it.

References

1. Zbik, M.; Smart, R. St C Miner Eng 2002, 15, 277.
2. Kogure, T.; Kameda, J.; Matsui, T.; Miyawaki, R. Am Miner 2006, 91, 1363.
3. Zhou, X.; Xie, X.; Yu, Z.; Mai, Y. Polymer 2007, 48, 3555.
4. Wu, G.; Wen, B.; Hou, S. Polym Int 2004, 53, 49.
5. Denac, M.; Musil, V.; Šmit, I. Compos A 2005, 35, 1282.
6. Garcia-Martinez, J. M.; Laguna, O.; Collar, E. P. J Polym Eng 1997, 17, 269.
7. Taranco, J.; Garcia-Martinez, J. M.; Laguna, O.; Collar, E. P. J Polym Eng 1994, 13, 287.
8. Lee, H.; Fasula, P. D.; Rodgers, W. R.; Paul, D. R. Polymer 2005, 46, 11673.
9. Lee, H.; Fasula, P. D.; Rodgers, W. R.; Paul, D. R. Polymer 2006, 47, 3528.
10. Kim, D. H.; Fasula, P. D.; Rodgers, W. R.; Paul, D. R. Polymer 2007, 48, 5308.
11. Kim, D. H.; Fasula, P. D.; Rodgers, W. R.; Paul, D. R. Polymer 2007, 48, 5960.
12. Kim, D. H.; Fasula, P. D.; Rodgers, W. R.; Paul, D. R. Polymer 2008, 49, 2492.
13. Available at: http://www.spartech.com
14. Available at: http://www.ides.com/grades/ds/E90354.htm
15. Yoon, P. J.; Hunter, D. L.; Paul, D. R. Polymer 2003, 44, 5341.
16. Cui, L.; Ma, X.; Paul, D. R. Polymer 2007, 48, 6325.
17. Solomon, O. F.; Ciuta, I. Z. J Appl Polym Sci 1962, 6, 683.
18. Delpech, M. C.; Coutinho, F. M. B.; Habibe, M. E. S. Polym Test 2002, 21, 155.
19. Bikiaris, D. N.; Achilias, D. S. Polymer 2008, 49, 3677.
20. Brandrup, J.; Immergut, E. H. Polymer Handbook; Wiley: New York, 1989.
21. Cheng, T. W.; Keskkula, H.; Paul, D. R. Polymer 1992, 33, 1606.
22. Cheng, T. W.; Keskkula, H.; Paul, D. R. J Appl Polym Sci 1992, 45, 1245.
23. As'habi, L.; Jafari, S. H.; Baghaei, B.; Khonakdar, H. A.; Pötschke, P.; Böhme, F. Polymer 2008, 49, 2119.
24. Wu, J.; Chen, Y.; Shen, Z.; Huang, J.; Chen, N. J Mater Sci Lett 1999, 18, 461.
25. Halpin, J. C. J Comp Mater 1969, 3, 732.
26. Halpin, J. C.; Affidl, J. L. K. Polym Eng Sci 1976, 16, 344.
27. Fras, I.; Boudeulle, M.; Cassagnau, P.; Michel, A. Polymer 1998, 39, 4773.
28. Yoon, P. J.; Fornes, T. D.; Paul, D. R. Polymer 2002, 43, 6727.
29. Yoon, P. J.; Hunter, D. L.; Paul, D. R. Polymer 2003, 44, 5323.